

# Experimental Evaluation of Calculation Models Used in In-Cylinder Flow Field Computations

Y.Moriyoshi

Department of Mechanical Engineering  
Chiba University  
1-33 Yaoi-cho, Inage-ku, Chiba 263  
Japan

## ABSTRACT

In order to numerically predict the in-cylinder phenomenon of IC engines, it is necessary to develop a mathematical model which can predict the in-cylinder flow field precisely. The author has been working to evaluate and modify turbulence models by making comparisons between calculations and measurement. In this study, three new models, the Rapid-distortion-theory incorporated k-ε model, the renormalization-group based k-ε model and the two-scale k-ε model are employed and their predictability is tested.

## INTRODUCTION

Since the in-cylinder flow field of IC engines is of complicated turbulence and compression-expansion occurs in a very short time, it is necessary to use mathematical models, which are evaluated by detailed measurements, to predict such a flow field. The author has made numerical calculations of six kinds of flow fields shown in Table 1 with initial values obtained by LDV measurements using a transparent cylinder engine. By comparing calculated values with measured values, estimations and modifications of turbulence models have been made. [1-5]

In the experiments, the turbulence component is defined as the high frequency component over a cut-off frequency in each engine-cycle to remove the cycle-to-cycle variation component, and the turbulence intensity is defined as its rms value.

Table 1. Tested flow fields by LDV ( Case I to VI )

|            | Axisymmetrical Field |              | 3-D Field   |
|------------|----------------------|--------------|-------------|
|            | Flat Piston          | W/Cavity     | Flat Piston |
| Low Swirl  | Solid-Vortex [I]     | Solid [III]  | Solid [V]   |
| High Swirl | Rankine-Vortex [II]  | Rankine [IV] | Solid [VI]  |
| Start CA   | 100deg BTDC          | 150deg BTDC  | ←           |
| End CA     | 90deg ATDC           | 90deg ATDC   | ←           |

Calculations are made on the cylindrical coordinate system using the SOLA method and hybrid scheme of the

Table 2. Specifications of model engine

|                       | Axisymmetrical Field |             | 3-D Field    |
|-----------------------|----------------------|-------------|--------------|
|                       | Pancake              | W/Cavity    | Pancake      |
| Displacement Vol.     | 402 cc               |             |              |
| Bore x Stroke         | 80 x 80 mm           |             |              |
| Top-Clearance         | 20.0mm               | 1.0mm       | 20.0mm       |
| Compression Ratio     | 5.0                  | 8.3         | 5.0          |
| Intake-valve Open     | 30deg BTDC           |             |              |
| Close                 | 30deg ABDC           |             |              |
| Exhaust-valve Open    | 30deg BBDC           |             |              |
| Close                 | 30deg ATDC           |             |              |
| Con-rod Length        | 200 mm               |             |              |
| Valve Diameter        | 32.0mm x 1           |             | 28.0mm x2    |
| Max. Valve-lift       | 8.4mm                |             | 6.0mm        |
| Swirl Ratio           | 1.5(LS) / 3.6(HS)    |             | LS / HS      |
| Cal. Mesh (r x θ x z) | 20 x 1 x 20          | 40 x 1 x 26 | 20 x 12 x 20 |

Table 3. Predictability of each turbulence model

|             | I | II | III & IV | V & VI |
|-------------|---|----|----------|--------|
| Std. k-ε    | ○ | ×  | ×        | △      |
| CD k-ε      | ⊙ | ×  | ×        | ○      |
| Rf k-ε      | × | ○  | ×        | —      |
| ARS         | ⊙ | △  | —        | —      |
| Rf + ARS    | ⊙ | ⊙  | ○        | ○      |
| RDT k-ε     | ⊙ | ×  | ×        | ○      |
| RNG k-ε     | ⊙ | ×  | ×        | ○      |
| 2-Scale k-ε | ⊙ | ⊙  | ○        | ○      |

⊙: Mean velocity and turbulence predictable

○: Only mean velocity predictable

△: Mean velocity qualitatively predictable

×: Poor predictability, —: N/A

second-order upwind and the central differencing for discretization. For the boundary condition, a near-wall model based on the wall-law is used. The specifications of the model engine and obtained results using several kinds of turbulence models are shown in Tables 2 and 3, respectively. The profile of the combustion chamber at TDC is sketched in Fig. 1.

The standard k- $\epsilon$  turbulence model ( including a term of divergence proposed by Morel[6] with a coefficient of  $C_3=1.373$  ) can predict the mean velocity in a flow field where nearly solid-vortex-like swirl exists, but cannot predict the turbulence characteristics. When the coefficient,  $C_D$ , which appears to express the eddy viscosity,  $\nu_t (=C_D k^2/\epsilon)$ , is changed as a function of the turbulence Reynolds number,  $Ret(=k^{1/2}L/\nu)$ , both the mean velocity and turbulence intensity can be predicted well on a nearly isotropic flow field like Case-I. This model will be called "CD-modified model".

In Case-II, which has a Rankine-vortex-like swirl, the standard or CD-modified model cannot predict the mean velocity nor turbulence characteristics, whereas another modified k- $\epsilon$  model using the flux Richardson number,  $R_f$ , in which the coefficient  $C_1$  in the  $\epsilon$  equation is changed by  $R_f$  times a newly introduced coefficient  $C_4$ , can predict only the mean velocity. However, because  $C_4$  is optimized for the Case-II flow field, this model cannot predict other flow fields. This model will be called an "Rf model".

Further, although the algebraic Reynolds stress (ARS) model, which is a simplified model from the Reynolds stress equation model, shows slight improvement in prediction compared to the standard k- $\epsilon$  model, drawbacks such as the calculation instability and inadequate preservation ability are apparent.

Therefore, the author tried to combine the ARS model with the Rf model. First, the degree of anisotropy was detected by using the ARS model. Next, the coefficient of  $C_4$  in the Rf model was determined according to the degree of anisotropy. This model predicts the mean velocity in

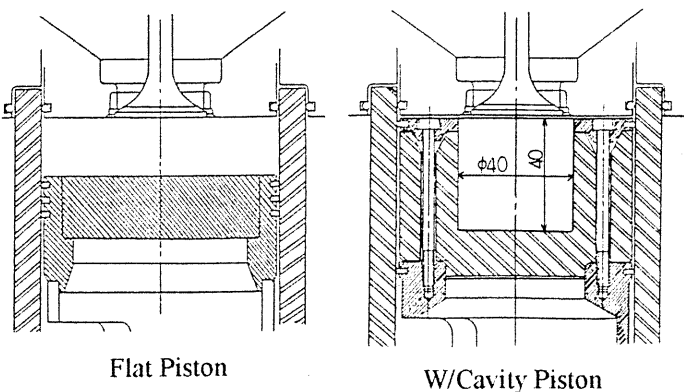


Fig. 1. Combustion chamber profile at TDC

every case as shown in Table 3. The model predicts the turbulence characteristics in Case-I and II. However, two problems that the ARS model itself cannot predict the Case-II well and that the model does not satisfy the "Galilean invariance" prevent us from using this combined model.

Because of these problems, recently noticed models such as the RNG (Re-Normalization Group) model[7], two-scale k- $\epsilon$  model[8] and RDT (Rapid Distortion Theory) incorporated k- $\epsilon$  model[6] are experimentally evaluated in the following section.

## TURBULENCE MODEL

### RDT incorporated k- $\epsilon$ model

Incorporation of the RDT into the k- $\epsilon$  model is discussed by Morel et. al.[6] According to Morel et. al., the coefficient  $C_3$  in the k- $\epsilon$  Eq.(1) is determined by the compression-type,  $n$  ( $n=1$ : uniaxial,  $n=2$ : cylindrical,  $n=3$ : spherical ) as in Eq.(2).

$$\frac{D(\rho k)}{Dt} = P - \rho \epsilon + \frac{\partial}{\partial x_i} \left( \frac{\mu_t}{\sigma_k} \frac{\partial k}{\partial x_i} \right)$$

$$\frac{D(\rho \epsilon)}{Dt} = C_1 \frac{\epsilon}{k} P - C_2 \rho \frac{\epsilon^2}{k} + \frac{\partial}{\partial x_i} \left( \frac{\mu_t}{\sigma_\epsilon} \frac{\partial \epsilon}{\partial x_i} \right) + (1 - C_3) \rho \epsilon D \quad (1)$$

where,  $\mu_t = \rho C_D k^2/\epsilon$ ,  $P = 2\mu_t(S_{ij}S_{ij} - \frac{1}{3}D^2) - \frac{2}{3}\rho kD$

$$S_{ij} = \frac{1}{2} \left( \frac{\partial U_i}{\partial x_j} + \frac{\partial U_j}{\partial x_i} \right), \quad D = \text{div} \vec{U}$$

$$\sigma_k = 1.0, \quad \sigma_\epsilon = 1.3$$

$$C_3 = \frac{2}{3}(C_1'' - C_1), \quad C_1'' = 3 + \frac{3}{2n} \quad \dots(2)$$

That is, the compression-type is first determined by the local strain,  $S_{ij}$ , after which  $C_3$  will be decided. Morel recommended  $n=1$ ,  $C_1 = 1.44$ ,  $C_2 = 1.92$  and  $C_3 = 1.373$ . The standard k- $\epsilon$  model employed in this study uses these values. Here, it is possible to change  $C_3$  locally by calculating the local strain  $S_{ij}$ , using Eq.(3).

$$a = 3(S_{11}^2 + S_{22}^2 + S_{33}^2) / (|S_{11}| + |S_{22}| + |S_{33}|)^2 - 1$$

$$n = 3 - \sqrt{2a} \quad \dots(3)$$

This model will be called as the RDT model.

### RNG k- $\epsilon$ model

The RNG method is an approach which has led to remarkable successes in the description of the phase transition phenomenon. In this approach, an expansion is made about an equilibrium state with known Gaussian statistics by making use of the correspondence principles wherein the effects of mean strains are represented by a random force. Bands of high wave numbers are systematically removed and space is rescaled.[7] By adapting this technique to the k- $\epsilon$  model, the following coefficients can be drawn.

$$C_1 = 1.42 - \frac{\eta(1 - \eta/\eta_0)}{1 + \beta\eta^3}, C_2 = 1.68, \sigma_k = \sigma_\varepsilon = 0.718$$

$$\text{where, } \eta = Sk/\varepsilon, S = (2S_{ij}S_{ji})^{1/2}, \eta_0 = 4.38, \beta = 0.015$$

When  $\eta$  becomes strong,  $C_1$  and then  $\varepsilon$  increase, but the eddy viscosity decreases as a result. It is possible to include the low Reynolds number effect near the wall. However, because  $CD$  is changed by a function of  $Ret$  to incorporate the low Reynolds number effect, this extension is not included in this study.

### Two-scale k- $\varepsilon$ model

In a flow field, where the turbulence energy generation is suddenly switched off, there is no necessity for  $\varepsilon$  to decrease immediately since the transportation of energy from the energy-containing-eddy to small eddies does not fall to zero. Thus, the energy from the energy-containing-eddy to small eddies does not fall to zero. Thus, the energy dissipation rate responds slowly to the applied mean strain.

In the standard k- $\varepsilon$  model, the coefficients are experimentally determined in simplified flow fields. Therefore, it might be inadequate to apply this model for such flow fields where a rapid compression-expansion occurs and the equilibrium of turbulence energy is not necessarily satisfied. Incorporating the idea of RDT probably enables the global effect on the turbulence enhancement or the decay by means of compression or expansion. However, the effect of the rapid local change of both the mean velocity (this can be expressed by the Reynolds number), and the turbulence characteristics (this can be expressed by the turbulence Reynolds number) by compression or expansion is not implied in this standard model.

For such a flow field with a rapidly changing  $Re$  and  $Ret$ , Hanjalic[8] discussed the two-scale k- $\varepsilon$  model. In this model, the turbulence energy supply is not at equilibrium with its dissipation. That is, two time scales of  $\varepsilon_p / k_p$  and  $\varepsilon_t / k_t$  exist where  $\varepsilon_p$  and  $k_p$  are the energy leaving rate from the "production region" and the energy contained in the "production region", respectively.  $\varepsilon_t$  and  $k_t$  are the dissipation rates in the smallest eddy region and the energy contained in the "transfer region" respectively. One must solve four equations to obtain these two time scales.

On the other hand, Chen et. al.[5] also incorporated two-scales into the k- $\varepsilon$  model. In this model, to deduce the terms of the  $\varepsilon$  equation, which include  $C_1$  and  $C_2$ , the Kolmogorov's time scale,  $(\nu^3/\varepsilon)^{1/4}$ , is employed instead of the original time-scale,  $k / \varepsilon$ . This model need not determine more additional coefficients, but  $C_1$  and  $C_2$  become functions of  $Re$  in his model.

Trying to introduce the former two-scale model into the in-cylinder flow calculation, one needs to determine the coefficients. This brings lack of universality and an increase in the calculation time. The latter two-scale model also seems to need adjusting of the coefficients. Here, Chen

replaced time scales of both  $C_1$  and  $C_2$  with the Kolmogorov time scale. Because  $C_2$  was determined experimentally in an isotropically homogeneous turbulent flow field, the author assumed that  $C_2$  is unchanged, but  $C_1$  which is multiplied by the mean strain should be changed using the Kolmogorov time scale. As the term including  $C_1$  reads  $C_1 \frac{1}{t} u'_i u'_j \frac{\partial U_i}{\partial x_j}$ , time scale,  $t$ , was changed from  $t_L (= k / \varepsilon)$  to  $t_\eta (= (\nu^3/\varepsilon)^{1/4})$ . Then,  $t_\eta / t_L = \varepsilon^{1/2} \nu^{1/2} / k = CD^{3/8} / Ret^{1/2}$  (for,  $\varepsilon = CD^{3/4} k^{3/2} / L$ )  
New  $C_1 = 15 Ret^{1/2} / CD^{3/8}$ . "15" is an optimized value for the Case-I flow field. In the following calculations, "15" will be used as a constant.

### EVALUATION OF TURBULENCE MODELS BY EXPERIMENTS

#### Axisymmetrical pancake shaped combustion chamber with solid-vortex-like swirl flow (Case-I)

In this case, the  $CD$ -modified model succeeded in predictions of both the mean velocity and turbulence characteristics as show in Table 3. Both the RNG and RDT models showed almost the same predictability. Therefore, a nearly isotropic flow field with low engine speed was easy to predict by each model tested here.

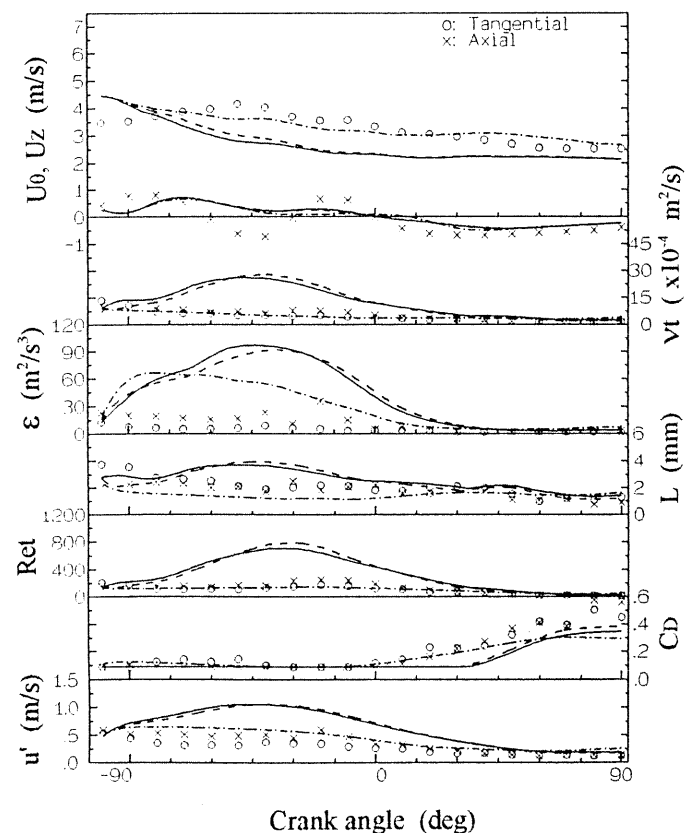


Fig. 2. Temporal variations of characteristic values at  $r=10, z=12\text{mm}$  (Case-II)  
(—: RDT model, - - -: RNG model, - · - ·: 2-Scale model)

Axisymmetrical pancake shaped combustion chamber with Rankine-vortex-like swirl flow (Case-II)

In this case, most of the models could not predict as shown in Table 3. The temporal variation of predictions at a point of  $r=10, z=12\text{mm}$  using the RDT, RNG and two-scale models is shown in Fig. 2. The axial and tangential measured values are plotted by marks of 'x' and 'o', respectively. Going top to bottom, the mean velocity of  $U_z$  and  $U_\theta$ , kinetic eddy viscosity,  $\nu_t$ , turbulence energy dissipation rate,  $\epsilon$ , integral length scale,  $L$ ,  $Re_t$ ,  $C_D$  and turbulence intensity,  $u'$  ( $u'_z$  and  $u'_\theta$  for experiments) are compared between the calculation and measurement.  $L$  was measured using the two-point simultaneous LDV technique. Experimental values of  $\nu_t$  and  $\epsilon$  were estimated by using expressions of  $\nu_t = C_D^{1/4} k^{1/2} L$  and  $\epsilon = C_D^{3/4} k^{3/2} / L$ , respectively.

It is obvious that the two-scale model shows better predictability compared to any other model. The quantitative agreement is, however, a little bit less than in Case-I.

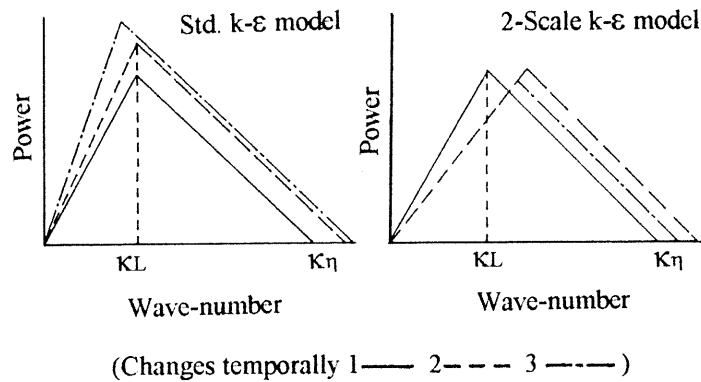


Fig. 3. Power spectrum profile of turbulence model

Further, the calculation result using the CD-modified model is almost the same with the RNG or RDT models.

Above results show that the RNG, RDT and CD-modified models cannot predict flow fields like Case-II, whereas the two-scale model can. Because the two-scale model can predict  $\nu_t$  and  $Re_t$  fairly well, the mean velocity and turbulence characteristics can be estimated well as a result. The value of  $Re_t$  is overestimated too much in other models, while its increase is appropriately controlled in the two-scale model because  $C_1$  is a function of  $Re_t$ . Although the two-scale model itself cannot take the anisotropy of flow field into account, it could predict the in-cylinder flow field by letting the Kolmogorov time scale change in accordance with  $Re_t$ . This implies that the main reason for the poor predictability of the standard  $k-\epsilon$  model is not the anisotropy of turbulence but the non-equilibrium of turbulence generation and dissipation. That is, regarding the spectrum profile shown in Fig. 3, in the standard  $k-\epsilon$  model, the peak power at the energy containing eddy's wave number,  $\kappa_L$ , and the maximum wave number,  $\kappa_\eta$ , increase with time as both  $k$  and  $\epsilon$  increase. On the other hand, in the two-scale model, because  $\kappa_L$  moves to the higher region,  $\epsilon$  increases slowly.

Axisymmetrical field with-cavity combustion chamber (Case-III & IV)

In this case, the predictability is much worse than the Case-II as shown in Table 3. Fig. 4 shows radial profiles of both the mean velocity and turbulence intensity in the axial and tangential directions. Three models of the RDT, RNG and two-scale are employed in the calculation. Regarding the axial component, predictions of the mean velocity are almost the same among the three at 70deg BTDC and its agreement with experiments is not bad. The turbulence intensity, however, is overpredicted by any model. At 20deg BTDC, an axially strong upwind flow is experimentally observed, but this quantitative prediction is not entirely

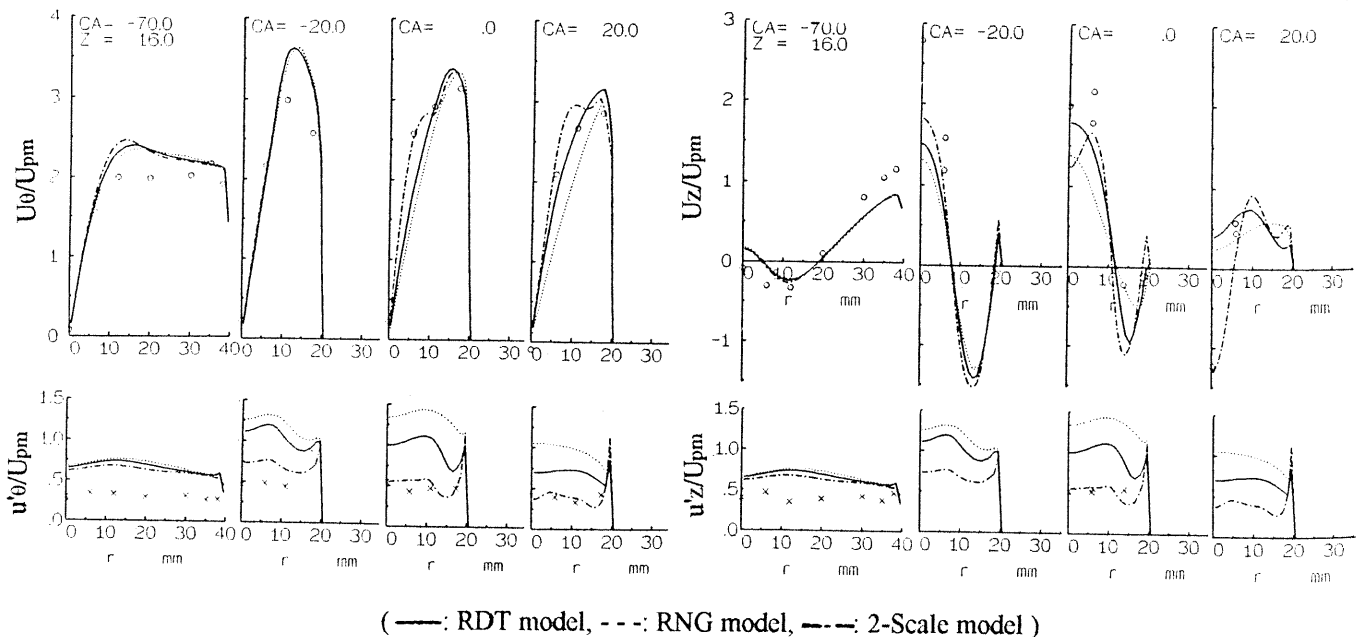


Fig. 4. Radial profiles of normalized mean velocity and turbulence intensity at  $z=16\text{mm}$

satisfactory. This is not only due to the turbulence model but also to the discretization scheme since quite strong shear flows exist inside the chamber and numerical errors might increase. Thus, the improvement of the discretization method should be done in such a complicated flow field. The measured turbulence intensity is not available at some period near the TDC because the piston-ring equipped at the top of the piston blocks the laser beam. After TDC, the two-scale model show the best predictability in both the mean velocity and turbulence intensity among the models. Further, the calculated result using the CD-modified model was almost the same with the RNG model.

### 3-D field with pancake shaped combustion chamber (Case-V & VI)

Although the combustion chamber is pancake-shaped like Case-I, the predictability of the 3-D field is inferior to the axisymmetrical one. For this reason, as the calculation is commenced with measured values as the initial condition, the insufficient space resolution of measurement makes the precision low. Moreover, since there exists a precession of swirl center in this 3-D field which is remarkable compared with the axisymmetrical one, the increase of the cycle-to-cycle variation contributes to this reason. Fig. 5 shows temporal variations of characteristic values at a point of  $r=30$ ,  $z=10\text{mm}$  using three models of the CD-modified,

RNG and two-scale. The RDT model could not predict the 3-D field because its calculation diverged.

The predictions of the mean velocity among the three models are almost the same, whereas the two-scale, RNG and CD-modified models show high predictability of turbulence characteristics compared with the experiments in this order. If the model which can treat the cycle-to-cycle variation phenomenon is incorporated, the degree of agreement will increase.[10] Therefore, it is possible to make the predictability improve in the 3-D field as well as in the axisymmetrical field by more detailed measurement and by taking into account the cycle-to-cycle variation phenomenon.

### Simulations at high engine speed

All experiments were made at low engine speed such as 320 or 640 r/min, which is quite low speed compared with the actual engine's speed. When the speed is increased, the turbulence intensity increases, but the integral length of turbulence, which strongly depends on the shape of the combustion chamber, does not change so much. So, both the  $Re$  and  $Ret$  increase relative to the engine speed and the state of flow field may change. Thus, only calculations from 150deg BTDC to 90deg ATDC are made at engine speed of 320 and 3200 r/min to see its effect in a with-cavity-piston configuration. The initial tangential mean velocity was set as a solid-vortex profile with a swirl ratio 1.5, and the radial

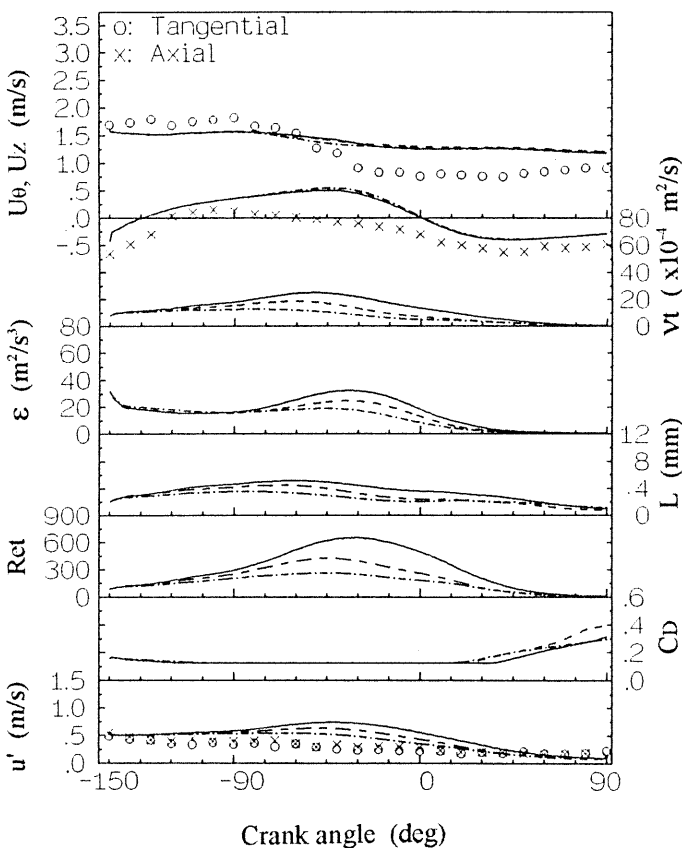


Fig. 5. Temporal variations of characteristic values at  $r=30$ ,  $z=10\text{mm}$  (Case-V)  
( —: CD-modified model, - - -: RNG model, - · - ·: 2-Scale model )

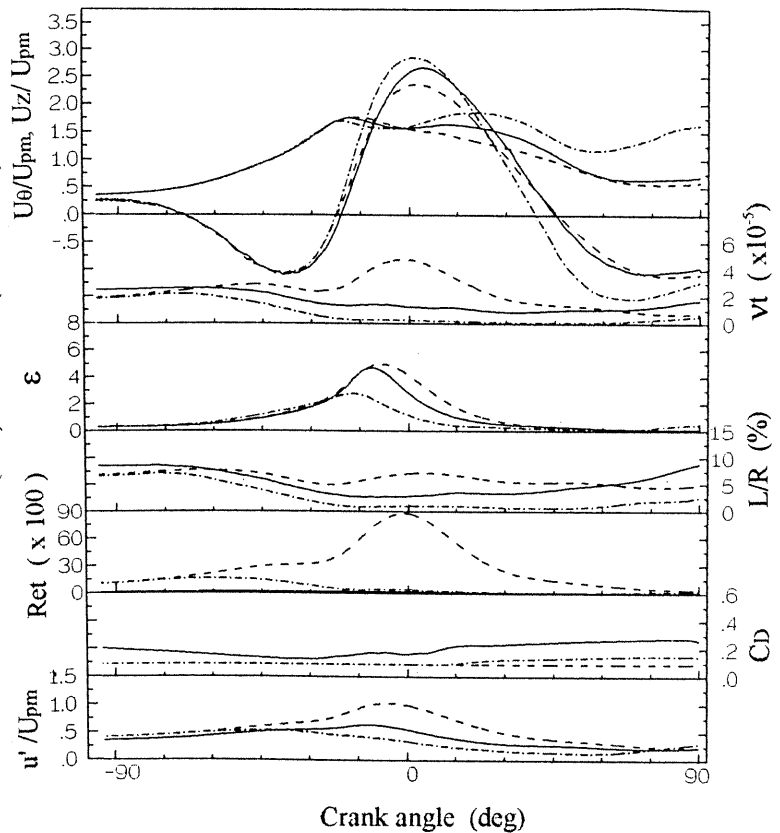


Fig. 6. Temporal variations of characteristic values at  $r=6$ ,  $z=16\text{mm}$  (Calculations Only)  
( —: 320r/min by 2-Scale model, - - -: 3200r/min by Std. model, - · - ·: 3200r/min by 2-Scale model )

and axial mean velocities of zero, turbulence intensity as 45% of the mean piston speed,  $U_{pm}$ , and turbulence length scale as 5% of cylinder radius,  $R$ , are given.

Fig. 6 shows temporal variations from 100deg BTDC to 90deg ATDC of characteristic values normalized by  $U_{pm}$  and  $R$  at a point of  $r=6$ ,  $z=16$ mm. Shown results are of i) two-scale model at 320 r/min, ii) standard  $k$ - $\epsilon$  model at 3200r/min and iii) two-scale model at 3200 r/min. The result using the RNG model at 3200 r/min is not shown as its calculation diverged around TDC. Further, the results between the RDT model and the standard model showed little difference quantitatively. Most of the characteristic values in the case of iii) are less than that of ii). This is probably due to the fact that in the two-scale model, the feedback by  $Ret$  that causes a larger value of  $\epsilon$  than in the standard model from 60deg BTDC brings about a decrease of  $k$ . Further, the effect of the engine speed can be observed between i) and iii), because the feedback effect is much stronger at the higher engine speed. An experimental evaluation, however, is still required.

## CONCLUSIONS

In order to precisely predict the in-cylinder flow field of IC engines, several kinds of turbulence models were employed in several kinds of flow fields and detailed comparison were made between the calculation and measurement. The following conclusions are offered.

- (1) In an isotropic flow field at low engine speed 320 r/min, the CD-modified  $k$ - $\epsilon$  model, RNG  $k$ - $\epsilon$  model and two-scale  $k$ - $\epsilon$  model can predict the mean velocity and turbulence characteristics quantitatively.
- (2) In the Rankine-vortex-like swirl flow field and strong shear flow field in a with-cavity combustion chamber at low engine speed, a newly proposed two-scale model shows the highest predictability in both the mean velocity and turbulence characteristics among the tested models.
- (3) By simulating a strong shear flow field at a high engine speed 3200 r/min using the two-scale model, differences of normalized values appear compared with the results at a low engine speed.

## ACKNOWLEDGMENT

The author would like to thank Prof. T. Kamimoto, Tokyo Institute of Technology for his help during the conception of this project and the staff at his laboratory for their experimental work. The author also thanks related companies for supporting this work.

## REFERENCES

- [1] Kamimoto, T., Moriyoshi, Y., Yagita, M., and Kobayashi, H., "Experimental Evaluation of Mathematical Models for Calculating In-Cylinder Air Motion with a Transparent Cylinder Engine," Heat & Mass Transfer in Gasoline & Diesel Engines, Hemisphere Publisher, pp. 485-496, 1989.
- [2] Moriyoshi, Y., Kamimoto, T., and Kobayashi, H., "Experimental Evaluation of  $k$ - $\epsilon$  Turbulence Model in Numerical Simulation of In-Cylinder Air Motion," JSAE Review Vol.10, pp. 10-16, 1989.
- [3] Moriyoshi, Y., Kamimoto, T., and Yagita, M., "Modification of  $k$ - $\epsilon$  Model in Anisotropic In-Cylinder Flows, Trans. Jpn. Sci. Mech. Eng., (in Japanese) Vol.58B, pp. 2314-2320, 1992.
- [4] Moriyoshi, Y., Yamaguchi, S., Kamimoto, T., and Yagita, M., "Numerical Analysis of 3-D In-Cylinder Flow and its Experimental Evaluation," Trans. Jpn. Sci. Mech. Eng., (in Japanese) Vol.58B, pp. 2617-2623, 1992.
- [5] Moriyoshi, Y., Kamimoto, T., and Yagita, M., "Definition of Turbulence in In-Cylinder Flow Fields," JSME Int. J., Vol.36B, pp. 172-177, 1993.
- [6] Morel, T. and Mansour, N.N., "Modeling of Turbulence in Internal Combustion Engines", SAE Paper No. 820046, 1982.
- [7] Yakhot V., and Orszag S.A., "Development of Turbulence Models for Shear Flows by a Double Expansion Technique," Phys. Fluids Vol.4A, pp. 1510-1520, 1992.
- [8] Hanjalik, K., Launder, B.E., and Schiestel, R., "Multiple-Time-Scale Concepts in Turbulent Transport Modeling," Proc. of 2nd Sympo on Turbulent Shear Flows, pp. 10.31-36., 1979.
- [9] Chen, C.J., and Singh, K., "Prediction of Buoyant Free Shear Flows by  $k$ - $\epsilon$  Model Based on Two Turbulence Scale Concept," Proc. of Int. Sympo. on Buoyant Flows pp. 26-36., 1986.
- [10] Moriyoshi, Y., Kamimoto, T., and Yagita, M., "Prediction of Cycle-to-Cycle Variation of In-Cylinder Flow in a Motored Engine," SAE Paper No. 9300669, 1993.